COBEM UBERLÂNDIA 2019

ABCM Associação Brasileira de Engenharia e Ciências Mecânicas

25th ABCM International Congress of Mechanical Engineering
October 20-25, 2019, Uberlândia, MG, Brazil

COB-2019-0905
THE INFLUENCE OF SMALL DEFECTS ON THE FATIGUE LIMIT OF 304L STAINLESS STEEL AT ROOM TEMPERATURE

Artur Lopes Dias
Departamento de Engenharia Mecânica, Universidade de Brasília – UnB, Brasília, DF, Brasil.
Instituto Federal de Brasília, Campus Estrutural, Brasília, DF, Brasil
artur.dias@ifb.edu.br

Cainã Bemfica de Barros
Fábio Comes de Castro
Departamento de Engenharia Mecânica, Universidade de Brasília – UnB, Brasília, DF, Brasil.
cainabemfica@gmail.com, fabiocastro@unb.br

Abstract. *This work investigates the influence of small defects on the fatigue limit of 304L stainless steel. Uniaxial fully reversed force-controlled and torque-controlled fatigue tests were carried out at room temperature in the presence of a cylindrical defect whose $\sqrt{area}$ is equal to 400 μm. Fatigue limit obtained from experimental data was 16% greater than the theoretical one obtained from the $\sqrt{area}$ parameter model, for both the uniaxial and torsional cases. Non-propagating cracks were not observed for experiments that did not fail after 2×10^6 cycles. The appearance and growth of fatigue crack were investigated. The cracks initiated close to the point of maximum principal stress at the hole surface, and propagated approximately in the plane perpendicular to the direction of the maximum principal stress.*

Keywords: *304L stainless steel, small defects, fatigue limit, $\sqrt{area}$ parameter model*

1. INTRODUCTION

Engineering components usually contain small defects, such as pits, scratches and non-metallic inclusions, whose dimensions are typically less than 1 mm. Processes such as casting, machining, heat treatment, shocks, corrosive environment can produce these small defects. These defects may act as stress raisers, which can reduce the fatigue resistance of these components. Hence, an investigation of the influence of small defects on the fatigue strength is important for a safer engineering design.

Murakami and co-workers have been developing a framework to predict the influence of small defects on fatigue strength (Murakami and Nemat-Nasser, 1983; Murakami and Endo, 1986; Yamashita *et al.*, 2018). They proposed that the fatigue limit in the presence of small defects is related to the square root of the project area of the defect on the plane normal to the loading axis ($\sqrt{area}$). Mathematically, the fatigue limit $\sigma_{\mathbf{w}}$ can be calculated as

$$\sigma_{\mathbf{w}} = \frac{1.43\,(HV+120)}{(\sqrt{area})^{\frac{1}{6}}} \tag{1}$$

Equation (1) was deduced based on the combination of the following two expressions:

$$K_{I\max} = 0.629\sigma_0\sqrt{\pi\sqrt{area}} \tag{2}$$

$$\Delta K_{\text{th}} = 3.3\times10^{-3}(HV+120)(\sqrt{area})^{\frac{1}{3}} \tag{3}$$

Equation (2) defines the maximum stress intensity factor ($K_{I\max}$) for surfaces defects with various shapes, under remote tensile stress (σ_0) (Murakami and Nemat-Nasser, 1983), while Eq. (3) defines the threshold stress intensity factor range (ΔK_{th}), under the stress ratio $R=-1$, based on the defect geometrical parameter ($\sqrt{area}$) and on a material parameter, Vickers Hardness (HV), for several engineering materials (Murakami and Endo, 1986). Equation (1) was developed for uniaxial loading and may be modified for other loading conditions. For torsional loading, the fatigue limit can be estimated as

$$\tau_{\mathbf{w}} = \frac{1}{(1-k)}\frac{1.43\,(HV+120)}{(\sqrt{area})^{\frac{1}{6}}} \tag{4}$$

where k is a constant that incorporates the effect of stress biaxiality (Endo, 2003). This modification is based on experimental observations that indicate that cracks tend to propagate perpendicular to the major principal stress direction near to the fatigue limit (Beretta and Murakami, 2000; Endo, 2003; Endo and Ishimoto, 2006; Schönbauer *et al.*, 2017b). At these critical planes, biaxial stresses are observed for torsional loading which, therefore, must be considered to estimate fatigue limit. For carbon steels, Cr-Mo steel, ductile cast irons, and high tension brass, values of k around -0.18 were observed (Schönbauer *et al.*, 2017b; Beretta and Murakami, 2000). Substituting k = -0.18 into Eq. (4), it follows that

$$\tau_{\mathbf{w}} = \frac{1.21\,(HV + 120)}{(\sqrt{area})^{\frac{1}{6}}} \tag{5}$$

Murakami's approach has been successfully applied to many materials (Murakami and Endo, 1986). Nevertheless, few works have addressed the influence of small defects on the fatigue strength of stainless steels (Ogura and Miyoshi, 1986; Guerchais *et al.*, 2015; Schönbauer *et al.*, 2017a,b; Chaves *et al.*, 2017).

The present work investigates the effect of small defects on the fatigue limit of 304L stainless steel. Uniaxial fully reversed force and torque-controlled fatigue tests were carried out on solid cylindrical specimens containing a cylindrical defect whose $\sqrt{area}$ is equal to 400 μm. The experimental data is used to evaluate the formula proposed by Murakami and Endo.

2. MATERIAL AND EXPERIMENTS

The 304L stainless steel was received as extruded bars with a diameter of 19.05 mm. The chemical composition of the material in weight percentage is 0.02% C, 18.16% Cr, 8.30% Ni, 1.34% Mn, 0.43% Si, 0.43% Si, 0.25% Cu, 0.22% Mo, 0.08% N, 0.03% P, 0.03% S, and Fe as balance. Bars were normalized at 1050 °C for 1 h to relieve residual stresses due to the extrusion process. Solid specimens were machined from the normalized bars and ground using sandpapers with grit numbers ranging from 220 to 2500. After grinding, a cylindrical small defect with an average diameter of 446 μm and height of 357 μm was produced at the center of each specimen by using a Computer Numerical Control machine with a 400 μm end mill. The geometry of the defect was investigated with an Olympus LEXT OLS4100 3D confocal laser microscope. Little variation from the target $\sqrt{area}$ value of 400 μm was observed between the samples holes, less than 3.75%.

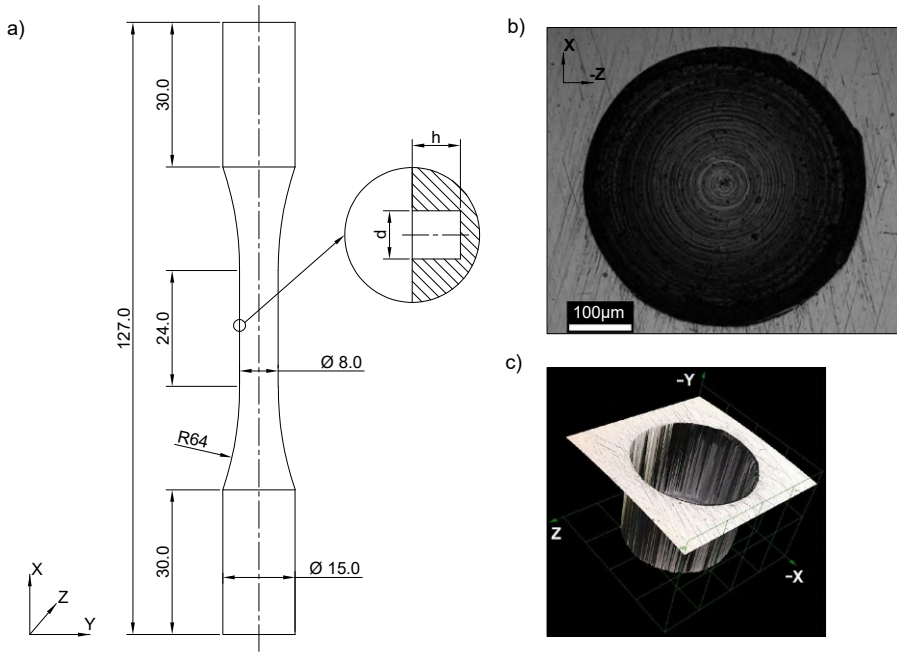

Figure 1. (a) Specimen and defect geometries (dimensions in mm); (b) Micrograph of the hole; (c) Hole 3D representation.

Figure 1a shows specimen dimensions used for fatigue tests, where d is the diameter and h is the height of the defect. Figures 1b and 1c show a picture and a three-dimensional representation of the hole, respectively. The mechanical properties of the 304L stainless steel are summarized in Table 1. Fully reversed force-controlled tension-compression and fully reversed torque-controlled fatigue tests were performed at room temperature in an MTS servo-hydraulic testing system. Fatigue tests were carried out until failure or run-out (2×10^6 cycles). Loading frequencies ranged from 1 Hz to 9

Table 1. Mechanical properties of the 304L stainless steel at room temperature

0.2 % Offset yield stress	Ultimate tensile strength	Reduction in area	Average grain size	Vickers Hardness
213 MPa	616 MPa	80%	44 μm	152 HV

Hz to avoid self-heating of the material. To monitor fatigue crack growth at the vicinity of the defect, one specimen for tension-compression and other for torsional was periodically inspected with a confocal microscope. The fracture surface of the tension-compression specimen was analysed using scanning electron microscope (SEM). Fatigue limit was defined as the greatest stress amplitude at which no failure occurs.

3. RESULTS AND DISCUSSION

Figure 2 shows the tension-compression fatigue test results for the three investigated stress amplitudes: 180 MPa, 170 MPa and 160 MPa. Solid symbols represent failed specimens and open symbols represent run-out specimens. For 170 MPa and 160 MPa failure did not occur, in contrast with the test carried out at 180 MPa, which failed after 1.1 x 10^5 cycles. Predicted fatigue limit according to Eq. (1) is represented in Fig. 2 by the red straight line.

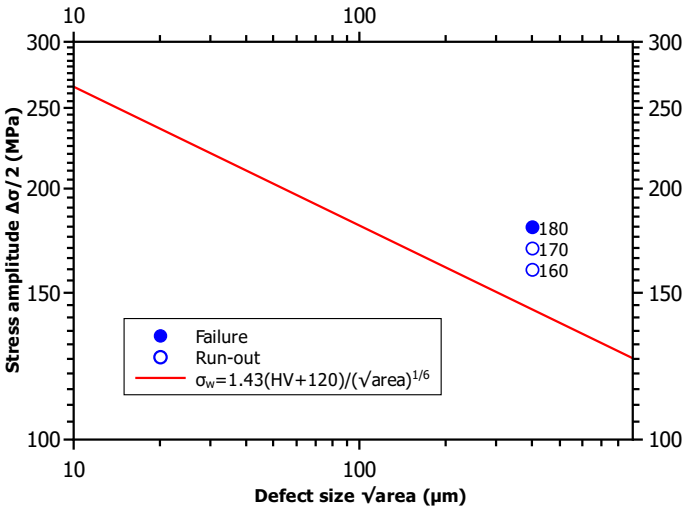

Figure 2. Stress amplitude vs. defect size for three tension-compression fatigue tests on 304L stainless steel.

Figure 3 shows the torsional fatigue test results for the three investigated stress amplitudes: 155 MPa, 145 MPa and 135 MPa. Solid symbols represent failed specimens and open symbols represent run-out specimens. For 145 MPa and 135 MPa failure did not occur, in contrast with the test carried out at 155 MPa, which failed after 5.0×10^5 cycles. Predicted fatigue limit according to Eq. (5) is represented in Fig. 3 by the straight line.

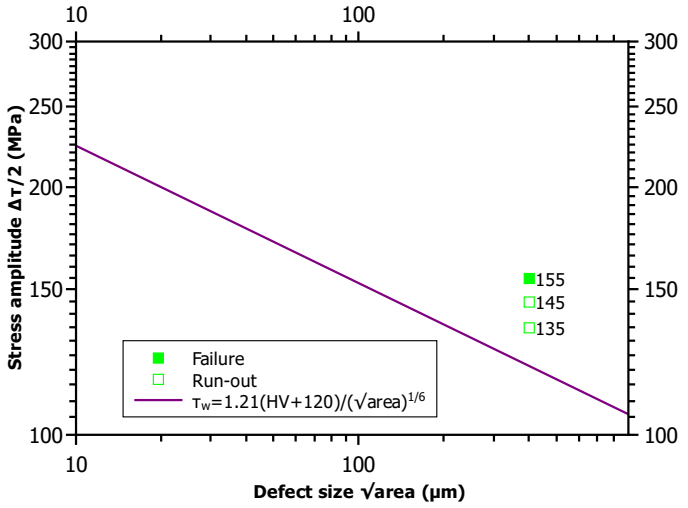

Figure 3. Stress amplitude vs. defect size for three torsional fatigue tests on 304L stainless steel.

The predicted fatigue limits for tension-compression and for torsional loading (143 MPa and 121 MPa, respectively) were 16% less than the experimental ones (170 MPa and 145 MPa, respectively). This level of accuracy is consistent with the results presented by Murakami and Endo (1986), in which the difference between predicted and experimental fatigue limits varied between -17.6% and -30.8% for two types of stainless steel, while for the other materials the difference was generally less than 10%. The ratio between the torsional and uniaxial fatigue limits ($\tau_{\mathbf{w}}/\sigma_{\mathbf{w}}$) of the 304L stainless steel was 0.85, which is similar to the ratio observed in the materials analysed by Beretta and Murakami (2000). It follows from this ratio that k in Eq. (3) is -0.18, similar to other materials previously investigated by Schönbauer *et al.* (2017b), and Beretta and Murakami (2000).

Figures 4a and 4b show fatigue cracks after $N = 2.34 \times 10^5$ cycles for the test performed at the stress amplitude of 180 MPa ($N_f = 2.84 \times 10^5$ cycles). In this test the frequency ranged from 1.5 Hz to 3.0 Hz in order to keep up with the growth of the crack. After 8×10^4 cycles a crack of 89 μm length was observed at the right side of the defect. From 10^5 cycles the crack growth was verified every 10^4 cycles up to 1.6×10^5 cycles. The measured values of the crack were: 220 μm, 301 μm, 429 μm, 486 μm, 543 μm, 612 μm and 702 μm. After 2.34×10^5 cycles a new crack 327 μm long was observed at the left side of the defect (Fig. 4b) while the one on the right was already 1185 μm long (Fig. 4a).

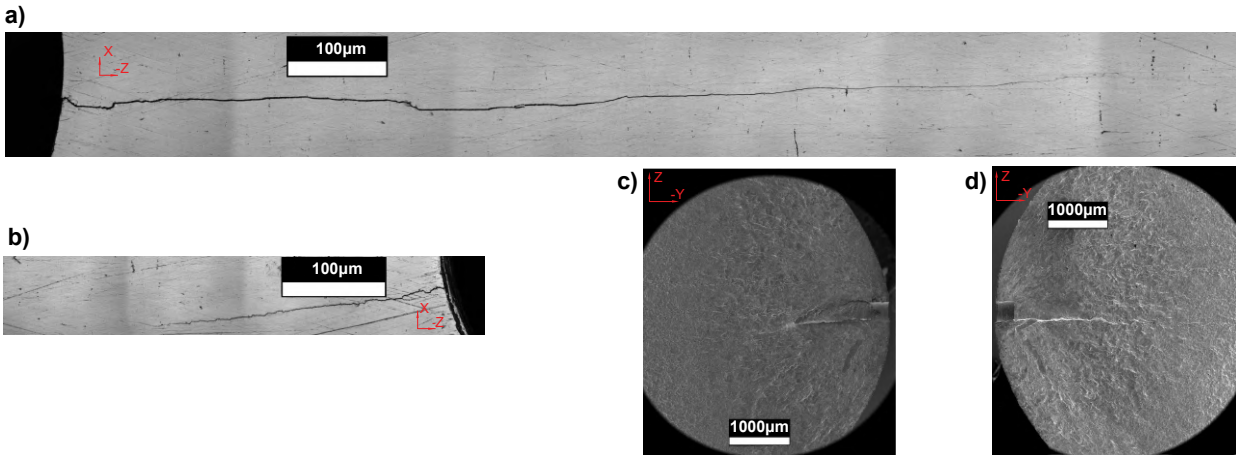

Figure 4. Cracking observation for the tension-compression test conducted at stress amplitude of 180 MPa. (a) Crack at the right side of the defect ($N = 2.34 \times 10^5$ cycles); (b) Crack at the left side of the defect ($N = 2.34 \times 10^5$ cycles); (c) and (d) SEM micrograph of the fracture surface.

Cracks initiated close to the point of maximum principal stress at the hole surface. They grew up approximately in the plane perpendicular to the direction of the maximum principal stress (90°). The crack that nucleated at the right side of the hole had a long propagation life, about 70% of the total life. It is possible to observe in SEM image (Fig. 4c and 4d) that other cracks nucleated in the internal part of the defect.

Figure 5 shows fatigue cracks after $N = 2.36 \times 10^5$ cycles for the test performed at the shear stress amplitude of 155 MPa. Fatigue cracks were observed both at the surface edge and at the bottom of the defect, with crack propagation occurring approximately at the plane perpendicular to the direction of the maximum principal stress. After 2.36×10^5 cycles, fatigue crack length was between 1009 μm and 1095 μm. Note that failure occurred only after 4.99×10^5 cycles, which implies that fatigue crack propagation is a significant part of total life, more than 53%.

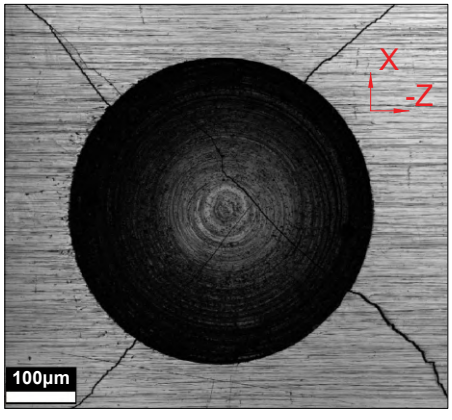

Figure 5. Cracking observation for the torsion test conducted at stress amplitude of 155 MPa ($N = 2.36 \times 10^5$ cycles).

For run-out experiments no cracks were observed by confocal microscopy, both for tension-compression and for torsional fatigue tests. This result agrees with the study of Ogura and Miyoshi (1986), that did not observe non-propagating cracks in fatigue tests at room temperature under fully-reversed loading of notched 304 stainless steel. According to the $\sqrt{area}$ model, the fatigue limit is not a critical condition for crack initiation, but is the threshold condition for the non-propagation of cracks (Murakami and Endo, 1983). In a rigorous way, the 304L and other stainless steels fall outside of the $\sqrt{area}$ parameter model because the non-propagating cracks were not detected (Murakami and Endo, 1986). However, the predicted fatigue limits have an acceptable accuracy from the engineering point of view.

4. CONCLUSIONS

Uniaxial fully reversed force-controlled and torque-controlled fatigue tests were carried out at room temperature in 304L stainless steel containing a cylindrical defect whose $\sqrt{area}$ is equal to 400 μm. Fatigue limit obtained from $\sqrt{area}$ parameter model was 16% less than the obtained from experimental data, both for tension-compression and for torsion. The ratio between the torsional and uniaxial fatigue limits was 0.85 and the parameter that represents the influence of stress biaxiality k was -0.18. Non-propagating cracks were not observed for experiments that did not fail after 2×10^6 cycles. Fatigue cracks were observed to initiate at the point of maximum principal stress at the hole surface. They propagated approximately in the plane perpendicular to the direction of the maximum principal stress, 90^{o} for tension-compression and 45^{o} for torsional fatigue tests.

5. ACKNOWLEDGEMENTS

Artur Lopes Dias would like to thank the support from Instituto Federal de Brasília -IFB. Fábio Castro acknowledges the support from the National Council for Scientific and Technological Development – CNPq (308126/2016-5 and 420677/2018-6) and the support from FAP-DF (0193.001583/2017). Cainã Bemfica would like to thank the support from the Coordination for the Improvement of Higher Education Personnel – CAPES.

6. REFERENCES

Beretta, S. and Murakami, Y., 2000. "Sif and threshold for small cracks at small notches under torsion". *Fatigue Fract. Engng. Mater. Str*, Vol. 23, No. 1, pp. 97–104.

Chaves, V., Beretta, G. and Navarro, A., 2017. "Biaxial fatigue limits and crack directions for stainless steel specimens with circular holes". *Engineering Fracture Mechanics*, Vol. 174, No. 1, pp. 139–154.

Endo, M., 2003. "The multiaxial fatigue strength of specimens containing small defects". *Biaxial/multiaxial fatigue fracture*, Vol. 31, No. 1, pp. 225–246.

Endo, M. and Ishimoto, I., 2006. "The fatigue strength of steels containing small holes under out-of-phase combined loading". *International Journal of Fatigue*, Vol. 28, No. 1, pp. 592–597.

Guerchais, R., Morel, F., Saintier, N. and Robert, C., 2015. "Influence of the microstructure and voids on the high-cycle fatigue strength of 316L stainless steel under multiaxial loading". *Fatigue & Fracture of Engineering Materials Structures*, Vol. 38, No. 1, pp. 1087–1104.

Murakami, Y. and Endo, M., 1983. "Quantitative evaluation of fatigue strength of metals containing various small defects or cracks". *Engineering Fracture Mechanics*, Vol. 17, No. 1, pp. 1–15.

Murakami, Y. and Endo, M., 1986. "Effects of hardness and crack geometries on ΔK_{th} of small cracks emanating from small defects". *K.J. Miller, E.R. de Los Rios (Eds.), The Behavior of Short Fatigue Crack, Mechanical Engineering Publications*, Vol. 1, No. 1, pp. 275–293.

Murakami, Y. and Nemat-Nasser, S., 1983. "Growth and stability of interacting surface flaws of arbitrary shape". *Engineering Fracture Mechanical*, Vol. 17, No. 3, pp. 193–210.

Ogura, K. and Miyoshi, Y., 1986. "Threshold behavior of small fatigue crack at notch root in type 304 stainless steel". *Engineering Fracture Mechanics*, Vol. 25, No. 1, pp. 31–46.

Schönbauer, B., Yanase, K. and Endo, M., 2017a. "The influence of various types of small defects on the fatigue limit of precipitation-hardened 17-4ph stainless steel". *Theoretical and Applied Fracture Mechanic*, Vol. 87, No. 1, pp. 35–49.

Schönbauer, B., Yanase, K. and Endo, M., 2017b. "Influences of small defects on torsional fatigue limit of 17-4ph stainless steel". *International Journal of Fatigue*, Vol. 100, No. 2, pp. 540–548.

Yamashita, Y., Murakami, T., Mihara, R., Okada, M. and Murakami, Y., 2018. "Defect analysis and fatigue design basis for ni-based superalloy 718 manufactured by selective laser melting". *International Journal of Fatigue*, Vol. 117, No. 1, pp. 485–495.

7. RESPONSIBILITY NOTICE

The authors are the only responsible for the printed material included in this paper.